Constitutively active Akt1 expression in mouse pancreas requires S6 kinase 1 for insulinoma formation

Samira Alliouachene,[1,2] Robyn L. Tuttle,[3] Stephanie Boumard,[1,2]
Thomas Lapointe,[1,2] Sophie Berissi,[1,2] Stephane Germain,[4] Francis Jaubert,[5]
David Tosh,[6] Morris J. Birnbaum,[3] and Mario Pende[1,2]

[1]INSERM U845, Paris, France. [2]Faculté de Médecine, UMRS-845, Université Paris Descartes, Paris, France.
[3]Howard Hughes Medical Institute and Department of Medicine, University of Pennsylvania School of Medicine, Philadelphia, Pennsylvania, USA.
[4]INSERM U833, College de France, Hôpital Européen Georges Pompidou, Paris, France. [5]Department of Pathology, Hospital Necker-Enfants Malades,
Paris, France. [6]Centre for Regenerative Medicine, Department of Biology and Biochemistry, University of Bath, Bath, United Kingdom.

Factors that promote pancreatic β cell growth and function are potential therapeutic targets for diabetes mellitus. In mice, genetic experiments suggest that signaling cascades initiated by insulin and IGFs positively regulate β cell mass and insulin secretion. Akt and S6 kinase (S6K) family members are activated as part of these signaling cascades, but how the interplay between these proteins controls β cell growth and function has not been determined. Here, we found that although transgenic mice overexpressing the constitutively active form of Akt1 under the rat insulin promoter (*RIP-MyrAkt1* mice) had enlarged β cells and high plasma insulin levels, leading to improved glucose tolerance, a substantial proportion of the mice developed insulinomas later in life, which caused decreased viability. This oncogenic transformation tightly correlated with nuclear exclusion of the tumor suppressor PTEN. To address the role of the mammalian target of rapamycin (mTOR) substrate S6K1 in the MyrAkt1-mediated phenotype, we crossed *RIP-MyrAkt1* and S6K1-deficient mice. The resulting mice displayed reduced insulinemia and glycemia compared with *RIP-MyrAkt1* mice due to a combined effect of improved insulin secretion and insulin sensitivity. Importantly, although the increase in β cell size in *RIP-MyrAkt1* mice was not affected by S6K1 deficiency, the hyperplastic transformation required S6K1. Our results therefore identify S6K1 as a critical element for MyrAkt1-induced tumor formation and suggest that it may represent a useful target for anticancer therapy downstream of mTOR.

Introduction

Pancreatic β cells in the islets of Langerhans are major nutrient sensors in mammals, as they produce and secrete the anabolic hormone insulin in response to nutritional cues. A defect of β cell function that causes insufficient insulin secretion is a common hallmark of all forms of diabetes mellitus and leads to hyperglycemia. Hence, factors promoting pancreatic β cell growth and function represent putative therapeutic targets against diabetes. Insulin itself and IGFs have been revealed as positive signals for insulin-producing β cells (1). Mouse mutants lacking both insulin and IGF1 receptors in pancreatic β cells develop severe diabetes due to defects in β cell mass and insulin secretion (2). Although the intracellular signal transduction from the transmembrane tyrosine kinase receptors is complex, genetic studies on mouse islet physiology have highlighted an important branch that starts from the phosphorylation of IRS1 and IRS2 by the receptors and leads to the activation of the serine threonine kinases Akt (also known as *PKB*) and S6K (S6 kinase). Compound mutations in the *IRS1* and *IRS2* genes sharply lower β cell mass and blood insulin levels (3). Deletion of S6K1 is sufficient to decrease β cell size and

insulin secretory capacity (4). Conversely, the constitutive activation of Akt1 upregulates β cell size and blood insulin levels; it also promotes β cell survival during cytotoxic stress (5, 6). However it is currently unclear whether Akt and S6K interact epistatically in the control of pancreatic β cell function or whether they act on parallel and redundant pathways.

In mammals, 3 distinct genes encode Akt homologs (*Akt1*, *Akt2*, and *Akt3*, which are also known as *PKBα*, *PKBβ*, and *PKBγ*, respectively), while 2 S6K genes exist (*S6K1* and *S6K2*) (7). Akt and S6K family members belong to the AGC class of kinases, sharing high sequence homology in the catalytic domain and similar recognition motifs in the target proteins. Thus Akt and S6K may have overlapping functions in the cell, as demonstrated by the existence of common substrates (8, 9). In addition, Akt and S6K kinase activities rely on similar regulatory mechanisms. Akt and S6K are activated by the same upstream kinases, PDK1 and mammalian target of rapamycin (mTOR), which respectively phosphorylate the activation loop and the hydrophobic motif sites (7). However, distinct mTOR partners direct phosphorylation toward Akt or S6K. The raptor-containing mTOR complex 1 (mTORC1) is responsible for S6K activation (10), while the rictor-containing mTOR complex 2 (mTORC2) phosphorylates Akt (11). Moreover, Akt and S6K can regulate each other. Akt positively increases S6K activity by multiple mechanisms, including the direct phosphorylation of the mTORC1 regulators tuberous sclerosis complex 2 (TSC2) and PRAS40, and indirectly increases S6K activity through the increase of intracellular energy and nutrient supplies (7). In contrast, S6K

---

participates in a feedback inhibitory loop that downregulates Akt action (12). Therefore, depending on the environmental conditions, cell types, and functional readout, the Akt- and S6K-signaling modules may operate upstream or downstream of each other or in parallel pathways.

Two tumor suppressors, the lipid phosphatase PTEN phosphatase and tensin homolog (PTEN) and the TSC heterodimer (TSC1/TSC2), coordinate the action of Akt and S6K on cell growth (7). PTEN counteracts the formation of phosphatidylinositol 3,4,5-triphosphate (PIP3), which plays an important role in the recruitment and activation of Akt at the membrane. TSC1/TSC2 switches the monomeric GTPase Rheb to a guanosine diphosphate–bound state that interferes with mTORC1 activity (13). While PTEN loss of function promotes Akt and consequently mTORC1/S6K signaling, TSC1/TSC2 loss of function directly upregulates mTORC1/S6K, leading to Akt inhibition due to the negative feedback mechanism (14, 15). Importantly, PTEN-null tumors are extremely sensitive to the macrolide antibiotic rapamycin, whose derivatives are currently in clinical trials as anticancer treatment (16, 17). Rapamycin primarily inhibits mTORC1 and thus affects multiple mTORC1 substrates in addition to S6K, including the eIF4E-binding proteins (4EBP1, 4EBP2, and 4EBP3). Moreover, long-term rapamycin treatment can also blunt mTORC2 signaling (18). It is therefore critical to determine the S6K contribution to the pleiotropic actions of Akt and mTOR on physiological and tumoral tissue growth.

Here, we set out to study the interplay between Akt and S6K in the regulation of pancreatic β cell growth and function. In addition, we address whether the constitutive activation of Akt/mTORC1/S6K may cause oncogenic transformation of β cells. We show that the expression of membrane-targeted Akt under the rat insulin promoter (RIP) triggers distinct growth responses in mouse pancreatic β cells. In addition to β cell hypertrophy, we also observed dysplasia, hyperplasia, and invasion in a subset of pancreas, leading to insulinoma formation in approximately 30% of the animals. This animal model of insulinoma, which we believe is novel, reproduced features of human disease, suggesting the Akt pathway as a crucial determinant in patients. Strikingly, S6K1 activity is not required for the Akt effects on β cell size but specifically affects β cell proliferation during the hyperplastic stage. Our results define S6K1 as a critical mTORC1 substrate that allows proliferation of insulinoma cells without affecting basal turnover of nontransformed β cells.

Results

The constitutively active form of Akt1 carrying a myristoylation signal (MyrAkt1) initiates multiple signal transduction pathways that mediate the pleiotropic effects of the enzyme on growth, survival, proliferation, metabolism, and tumorigenesis (19–22). In pancreatic β cells, the activation of the mTOR/S6K pathway by the *RIP-MyrAkt1* transgene was demonstrated by the increased phosphorylation of ribosomal protein S6 (rpS6), a substrate for S6K1 and S6K2 (Figure 1A). We have previously shown that *S6K1* gene deletion leads to hypoinsulinemia and β cell atrophy (4) as opposed to MyrAkt1-induced hyperinsulinemia and β cell hypertrophy (5, 6). To demonstrate whether S6K1 and MyrAkt1 alleles interact epistatically, we crossed the 2 mouse strains and compared the β cell function of the progeny with that of wild-type mice. First, we assessed whether *S6K1* deletion altered MyrAkt1 expression in β cells by immunoblot analysis with an antibody that

detected both endogenous and transgenic Akt. As shown in Figure 1B, the amount of MyrAkt1 was comparable in the pancreata of *RIP-MyrAkt1* and *RIP-MyrAkt1;S6K1−/−* mice, ruling out a variation of transgene expression as a function of the S6K1 genotype.

At 3 months of age, the *RIP-MyrAkt1* mice had 2.6-fold higher plasma insulin levels than controls, which accounted for the hypoglycemia in the fed and fasted states (Figure 1C) (5, 6). The *S6K1* deletion caused an approximately 35% reduction of plasma insulin levels in both MyrAkt1-positive and -negative mice (Figure 1C), suggesting a permissive role for S6K1 to sustain insulin secretion. Despite the lower plasma insulin levels as compared with *RIP-MyrAkt1* mice, the fed and fasting glucose levels were also decreased in *RIP-MyrAkt1;S6K1−/−* mice (Figure 1C). Moreover, the control of glycemia after an i.p. injection of glucose was improved in MyrAkt1-positive mice as compared with wild type but was not significantly affected by the *S6K1* genotype (Figure 1D). Altogether, these results suggest an increased insulin sensitivity in *S6K1*-deficient mice, as previously reported (12). To address insulin action in MyrAkt1-expressing mice, we measured glycemia after insulin administration and demonstrated that *RIP-MyrAkt1;S6K1−/−* mice were more insulin sensitive than *RIP-MyrAkt1* mice (Figure 1D). Reduced adiposity is likely to contribute to the amelioration of insulin action in *S6K1*-deficient mice (12), as suggested by the differences in total body weight depending on mouse genotypes (wild type, 31.7 ± 0.22 g; *S6K1−/−*, 23.9 ± 0.12 g; *RIP-MyrAkt1*, 32.9 ± 0.28 g; *RIP-MyrAkt1;S6K1−/−*, 24.6 ± 0.15 g). In conclusion, the *S6K1* deletion attenuates the positive effects of MyrAkt1 on insulin secretion while improving insulin sensitivity in peripheral tissues. The net result of these 2 opposite actions on glucose homeostasis is a mild hypoglycemic state during fasting and ad libitum feeding.

One of the primary consequences of MyrAkt1 expression in pancreatic β cells is a striking hypertrophy (5, 6) that may explain the increased capacity in insulin storage and release (23). In skeletal muscles, we have recently shown that S6K1 is required for the mTOR-dependent control of cell size by MyrAkt1 (24). To evaluate how MyrAkt1, mTOR, and S6K1 interact to regulate β cell growth, Glut2 immunostaining was performed to visualize β cell size in the different MyrAkt1/S6K1 mouse genotypes. Since a mosaic pattern of MyrAkt1 expression was observed in some islets of *RIP-MyrAkt1* and *RIP-MyrAkt1;S6K1−/−* mice, possibly due to transcriptional silencing of the transgene, pancreas sections were coimmunostained with anti–HA epitope tag antibodies to visualize MyrAkt1-positive cells (Figure 2A). As expected, *S6K1−/−* cells were 30% smaller than wild type, whereas HA-tagged MyrAkt1-expressing cells were 5 times larger. A similar analysis using anti–β catenin immunostaining confirmed these findings (Supplemental Figure 1A; supplemental material available online with this article; doi:10.1172/JCI35237DS1). These changes in β cell size largely accounted for the differences in β cell mass, which was reduced by half and increased by 3.5-fold in the *S6K1−/−* and *RIP-MyrAkt1* pancreata, respectively (Supplemental Figure 1B). Surprisingly, S6K1 deletion was not sufficient to reduce the size of MyrAkt1-positive cells (Figure 2A and Supplemental Figure 1). Since pancreatic β cells also express the S6K2 homologous gene, we asked whether a complete loss of function in the S6K pathway would affect MyrAkt1-induced β cell growth. As shown in Figure 2A, the combined deletion of S6K1 and S6K2 slightly reduced the size of MyrAkt1-expressing cells. However, the size of *RIP-MyrAkt1;S6K1−/−;S6K2−/−* cells was still 4-fold larger than those of wild-type control, suggesting that other MyrAkt1 effectors participate in this regulation independently of S6K activity.
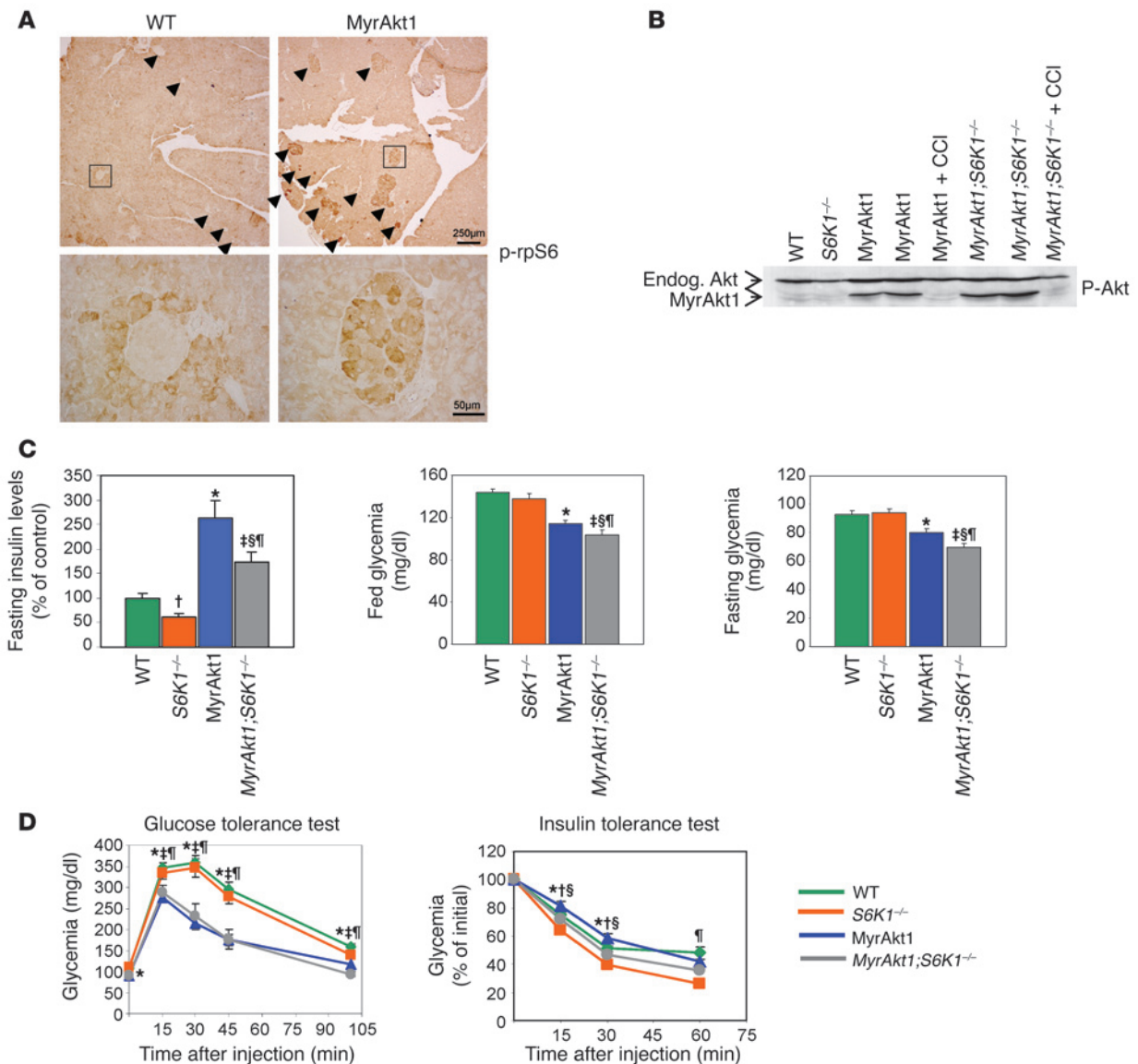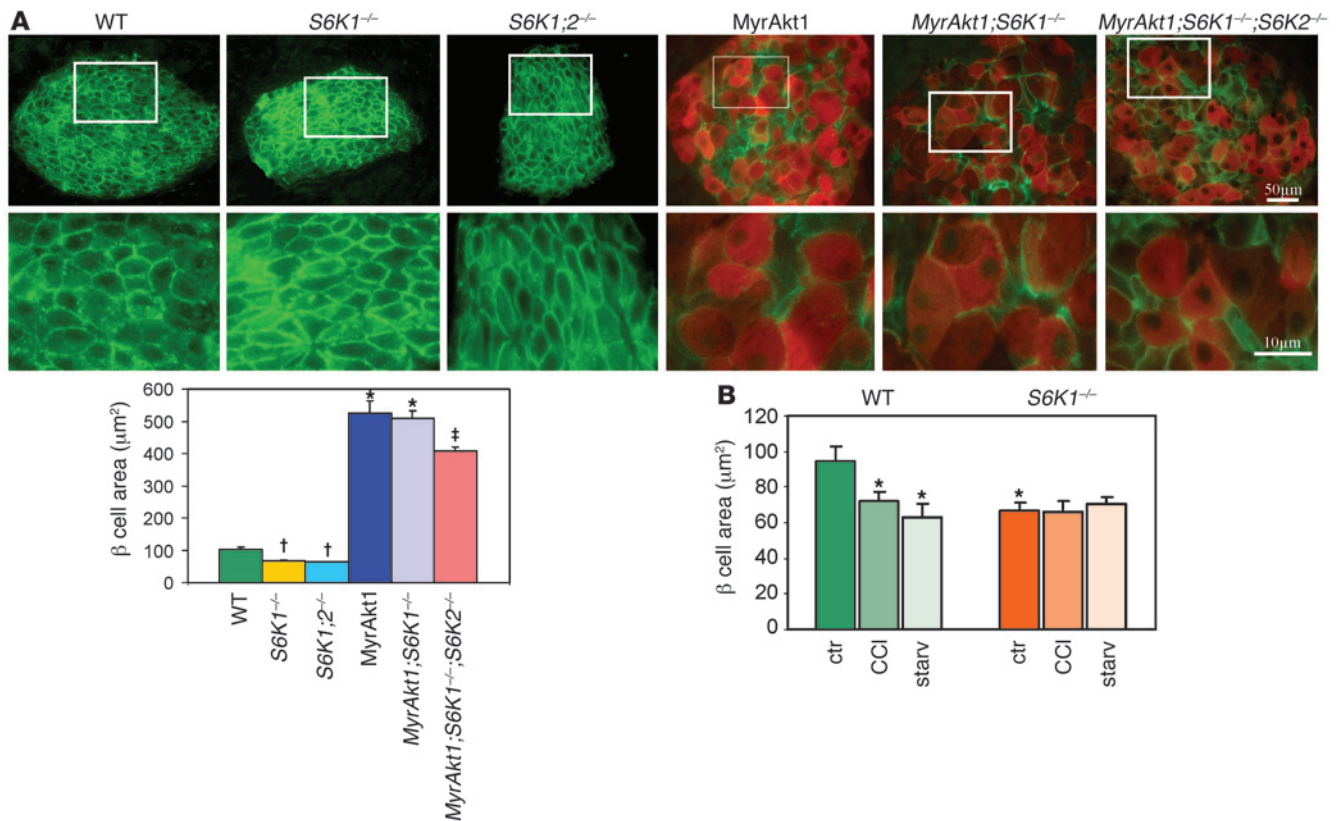
Figure 1
Effect of *S6K1* deletion on insulinemia and glycemia of *RIP-MyrAkt1* mice. (**A**) MyrAkt1 upregulates S6K activity in pancreatic β cells. Representative sections of pancreas immunostained with antibodies against phospho-rpS6 Ser235/236. Arrowheads indicate pancreatic islets. Scale bars: 250 μm (upper panels); 50 μm (lower panels). (**B**) Rapamycin treatment but not *S6K1* deletion shuts off *RIP-MyrAkt1* transgene expression. Immunoblot analysis of protein extracts from pancreata of the indicated genotype using anti-phospho Akt Ser473. Mice of the indicated genotype were 4 months old. Where indicated, mice were treated i.p. daily with 4.5 mg/kg of the rapamycin derivative CCI-779 (CCI) for 5 days. Endog., wild-type protein. (**C**) Insulinemia and glycemia. Mice of the indicated genotypes were fasted for 14 hours or randomly fed. Plasma insulin levels were measured by ELISA assay, blood glucose levels by a glucometer. Data represent mean ± SEM for at least 10 mice per genotype. *$P < 0.05$, wild-type versus MyrAkt1 mice; †$P < 0.05$, wild-type versus *S6K1⁻/⁻* mice; ‡$P < 0.05$, wild-type versus *MyrAkt1;S6K1⁻/⁻* mice; §$P < 0.05$, *MyrAkt1* versus *MyrAkt1;S6K1⁻/⁻* mice; ¶$P < 0.05$, *S6K1⁻/⁻* versus *MyrAkt1;S6K1⁻/⁻* mice. (**D**) Glucose and insulin tolerance tests. Mice were starved for 14 hours and treated i.p. with 2 g/kg glucose or 1 U/kg insulin. Data represent mean ± SEM for at least 10 mice per genotype.

The FOXO, GSK3, and 4EBP protein families may negatively regulate growth (25–27). MyrAkt1 relieves this inhibition by direct phosphorylation of FOXO and GSK3, by downregulating 4EBP expression, and by activating the 4EBP kinase mTOR (28, 29). As expected, GSK3 phosphorylation was upregulated while 4EBP expression was decreased in MyrAkt1-expressing islets (Supplemental Figure 2). Importantly, S6K1 deletion did not affect these responses. Under our culture conditions, we could not detect

changes in 4EBP phosphorylation depending on the islet genotype, as assessed by electromobility shift. Unfortunately, the FOXO phosphorylation could not be revealed by immunoblot analysis of islet extracts. To dissect the contribution of mTOR-independent and -dependent pathways in β cell growth, mice were treated for 5 days with the mTOR inhibitor and rapamycin derivative CCI-779 at a dose of 4.5 mg/kg or, alternatively, were nutrient starved for 2 days. Both treatments suppressed Ser235/236 rpS6 phosphorylation in
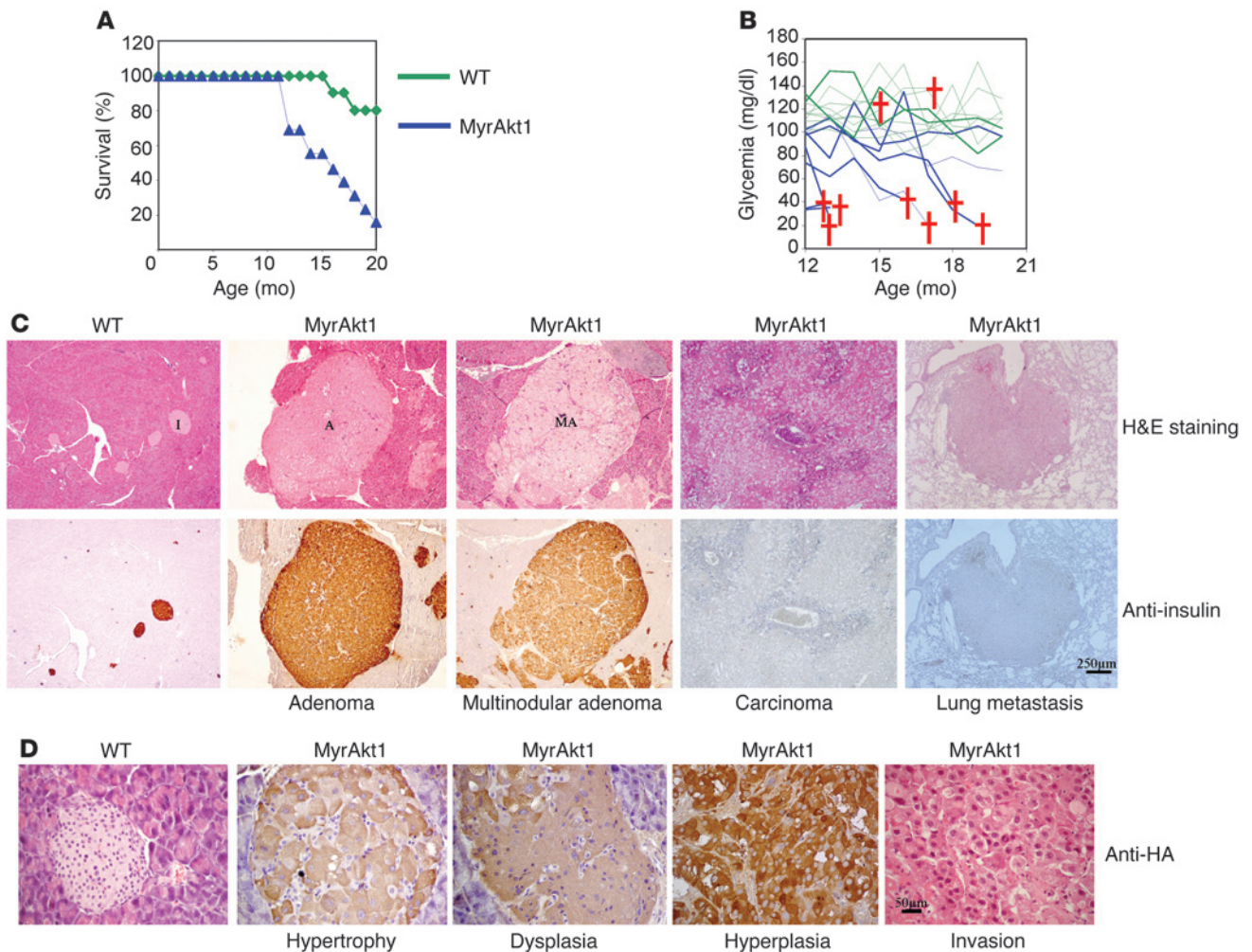
Figure 2
β cell growth control by MyrAkt1, nutrients, and the mTOR/S6K1 pathway. (**A**) MyrAkt1-induced β cell growth is not decreased in the absence of S6K1 activity. Representative sections of pancreas coimmunostained with antibodies against Glut2 (green) and HA to visualize MyrAkt1-expressing cells (red). Data represent mean ± SEM for at least 3 mice per genotype. In *MyrAkt1*, *MyrAkt1;S6K1⁻ᐟ⁻*, and *MyrAkt1;S6K1⁻ᐟ⁻;S6K2⁻ᐟ⁻* mice, the HA-positive cells were measured; in wild-type *S6K1⁻ᐟ⁻* and *S6K1⁻ᐟ⁻;S6K2⁻ᐟ⁻* mice, the Glut2-positive cells were measured. At least 200 cells were analyzed per mouse. (**B**) β cell size of *S6K1⁻ᐟ⁻* mice is not reduced by rapamycin and starvation. Mice were either starved (starv) for 2 days or treated i.p. daily with 4.5 mg/kg of the rapamycin derivative CCI-779 for 5 days. Cell size was measured by Glut2 immunostaining. Data represent mean ± SEM for at least 3 mice per genotype. *$P < 0.05$, wild-type versus MyrAkt1 and *MyrAkt1;S6K1⁻ᐟ⁻* mice; †$P < 0.05$ wild-type versus *S6K1⁻ᐟ⁻* and *S6K1⁻ᐟ⁻;S6K2⁻ᐟ⁻* mice; ‡$P < 0.05$ *MyrAkt1;S6K1⁻ᐟ⁻;S6K2⁻ᐟ⁻* versus MyrAkt1 and *MyrAkt1;S6K1⁻ᐟ⁻;S6K2⁻ᐟ⁻* mice. Ctr, control.

liver (data not shown), indicating that they were effective in inhibiting mTOR activity. CCI-779 decreased wild-type β cell size but did not further shrink *S6K1⁻ᐟ⁻* cells (Figure 2B). Similarly, *S6K1⁻ᐟ⁻* cells were resistant to nutrient starvation, while wild-type cells reduced their sizes to values comparable to those of S6K1 mutants (Figure 2B). Thus, *S6K1* deletion is sufficient to reproduce the effect of mTOR inhibition and nutrient depletion on β cell size. However, a role of the mTOR pathway in MyrAkt1-induced cell growth was not possible to assess, as CCI-779 shut off *MyrAkt1* transgene expression (Figure 1B). A likely explanation for this finding is the rapamycin sensitivity of the RIP that was used to drive *MyrAkt1* transcription (30). Of note, *S6K1* deletion did not mimic this effect of the rapamycin derivative (Figure 1B), indicating that mTOR interferes with insulin promoter–driven MyrAkt1 production through an S6K1-independent mechanism. In conclusion, S6K1 is required for the modulation of β cell growth by nutrients (Figure 2B) but is dispensable for MyrAkt1 action on cell size (Figure 2A).

After 1 year of age, the lethality rate was increased in *RIP-MyrAkt1* mice as compared with wild-type control (Figure 3A). Death was preceded by hypoglycemia, which suggested a deregulation of insulin production (Figure 3B). Histopathological analysis of old

RIP-MyrAkt1 mice revealed pancreatic islet tumors that maintained insulin expression in 19 out of 23 cases (Figure 3C). These insulinomas were classified as adenomas with rounded and encapsulated edges (10 out of 19 cases) or multinodular adenomas with partial loss of the fibrous capsule (9 out of 19 cases). The 4 remaining cases of pancreatic tumors were invasive carcinomas. One case of lung metastasis was observed in an 18-month-old tumor-bearing animal, while liver, kidney, and lymphatic tissues were not affected. Insulinomas were the likely cause of the observed hypoglycemia and lethality in the *RIP-MyrAkt1* mice. Importantly, another independent *RIP-MyrAkt1* transgenic mouse line also presented with β cell hypertrophy (5) and pancreatic endocrine neoplasia (Supplemental Figure 3), thus excluding a positional effect due to transgene insertion in the genome. As shown in Figure 3D, distinct features of islet growth and insulinoma formation were identified in pancreata from *RIP-MyrAkt1* mice as compared with control. In the totality of pancreas specimens, hypertrophy was observed in MyrAkt1-expressing islets, as defined by large β cells, which maintained an organized structure with well-defined margins. Cells had prominent nuclei with large nucleoli and were surrounded by dilated and asymmetric vessels. Seventy percent of pancreas
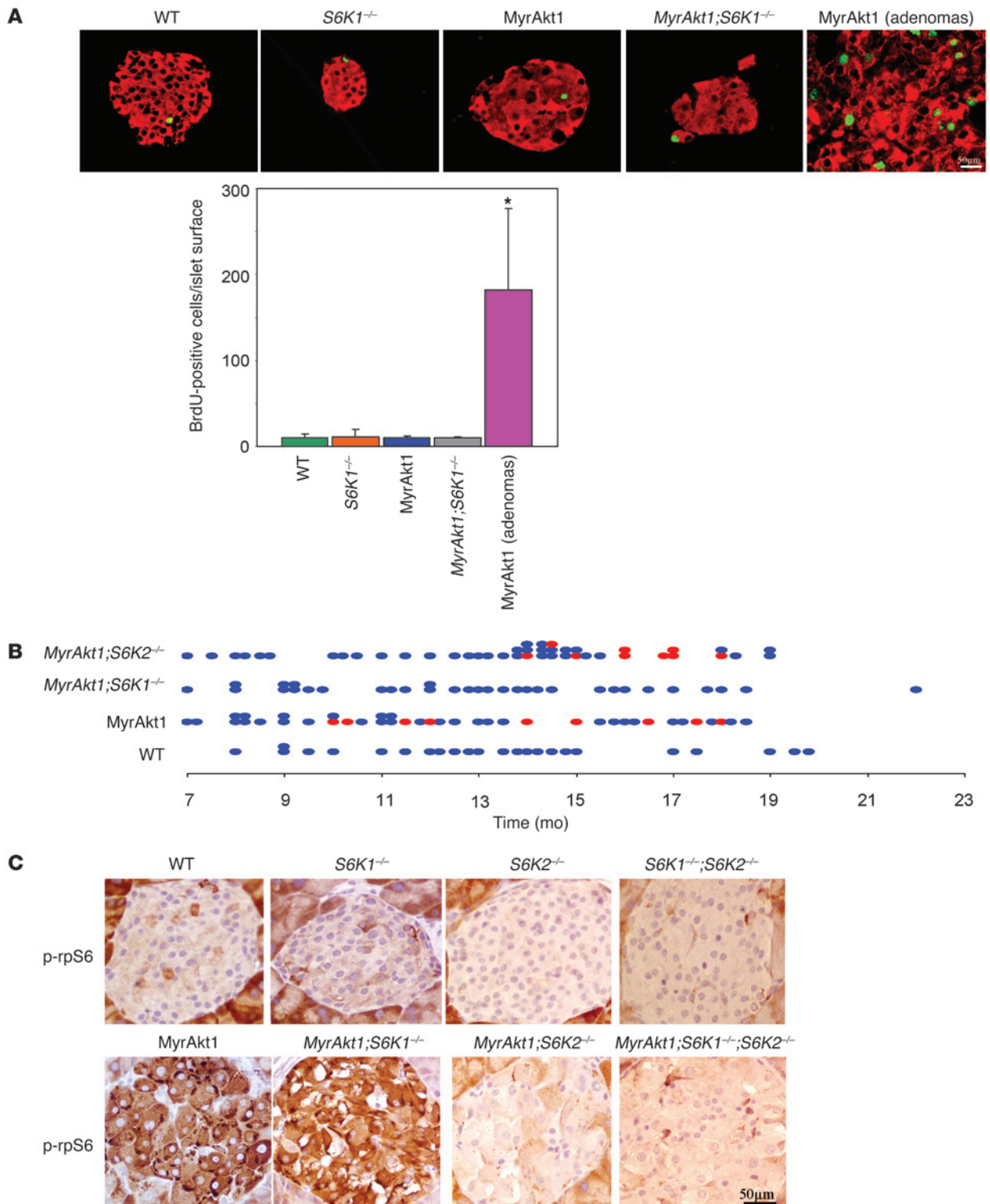
Figure 3
RIP-MyrAkt1 mice develop insulinomas. (**A**) Survival rate is decreased in *RIP-MyrAkt1* mice. Cohorts of animals (*n* = 10 for the control animals; *n* = 13 for the RIP-MyrAkt1 animals) were monitored over a period of 20 months to ascertain their lifespan. (**B**) Death of MyrAkt1 mice is preceded by a hypoglycemic state. Summary of the fed blood glucose levels for both the *RIP-MyrAkt1* animals and their wild-type cohorts over time, on the same graph. Cohorts of animals (*n* = 9 for mice of each genotype) were assayed monthly for their fed blood glucose levels over a span of 8 months. Each line represents an individual animal. Deaths of mice are represented by crosses. (**C**) Insulinoma formation in *RIP-MyrAkt1* mice. Sections of pancreas stained with H&E or immunostained with insulin. Representative images of islets (I), adenomas (A), multilobular adenomas (MA), carcinoma, and lung metastasis are shown. Scale bar: 250 μm. (**D**) Islet hypertrophy, dysplasia, hyperplasia, and malignant transformation in *RIP-MyrAkt1* mice. Representative sections of pancreata immunostained with the HA antibody to visualize MyrAkt1 expression and counterstained with hematoxylin. Scale bar: 50 μm.

specimens also displayed dysplastic islets with disorganized cells, irregular in shape and size. Peripheral or infiltrating fibrosis was also commonly observed in the islets, as evidenced by trichrome staining (Supplemental Figure 4). However, in hypertrophic and dysplastic islets, the proliferation of MyrAkt1-expressing pancreatic β cells did not differ from that of the control islets and remained lower than 0.5%, as assessed by BrdU incorporation after an 8-hour pulse (Figure 4A). In distinct hyperplastic islets, MyrAkt1-expressing tissues contained at least 5% of BrdU-positive cells and sharply increased their mass. Thus, MyrAkt1 triggers multiple growth responses with variable penetrance.

In the subset of pancreatic carcinoma and lung metastasis, tissue presented with BrdU-positive malignant tumor cells that were negative for HA-tagged MyrAkt1 and insulin expression (Figure 3, C

and D; Supplemental Figure 5). Moreover, these cells were also negative for neuroendocrine markers such as synaptophysin (data not shown). Scattered cells weakly expressing the homeodomain factor of the pancreatic lineage Pdx1 were observed in the lung metastasis (Supplemental Figure 5). Since MyAkt1 expression is under the control of the insulin promoter, these results suggest that carcinomas and metastasis may originate from insulin-expressing mature β cells that dedifferentiate as a consequence of MyrAkt1 expression and maintain malignant properties even after the shutoff of oncogene expression. Although we cannot exclude that malignant cells originate from non-MyrAkt1–expressing cells, this possibility is unlikely, as they were never observed in wild-type mice. In addition, the tissue displayed anatomopathological features of endocrine origin, including high vascularization and trabecular organization.

Figure 4
S6K1 deletion impairs β cell tumorigenesis. (**A**) β cell proliferation in distinct genotypes and during tumor progression. Representative sections of pancreata immunostained with antibodies against insulin (red) and BrdU to visualize proliferating cells (green). Histogram represents the mean ± SEM of islet or tumor BrdU incorporation for at least 3 mice per genotype. *$P < 0.05$ versus wild-type controls. Scale bar: 50 μm. (**B**) Mice of the indicated genotype were sacrificed at different ages and scored positive (red) or negative (blue) for the presence of insulinomas. (**C**) rpS6 phosphorylation in S6K mutants. Representative sections of pancreas immunostained with antibodies against phospho-rpS6 Ser235/236. Scale bar: 50 μm.
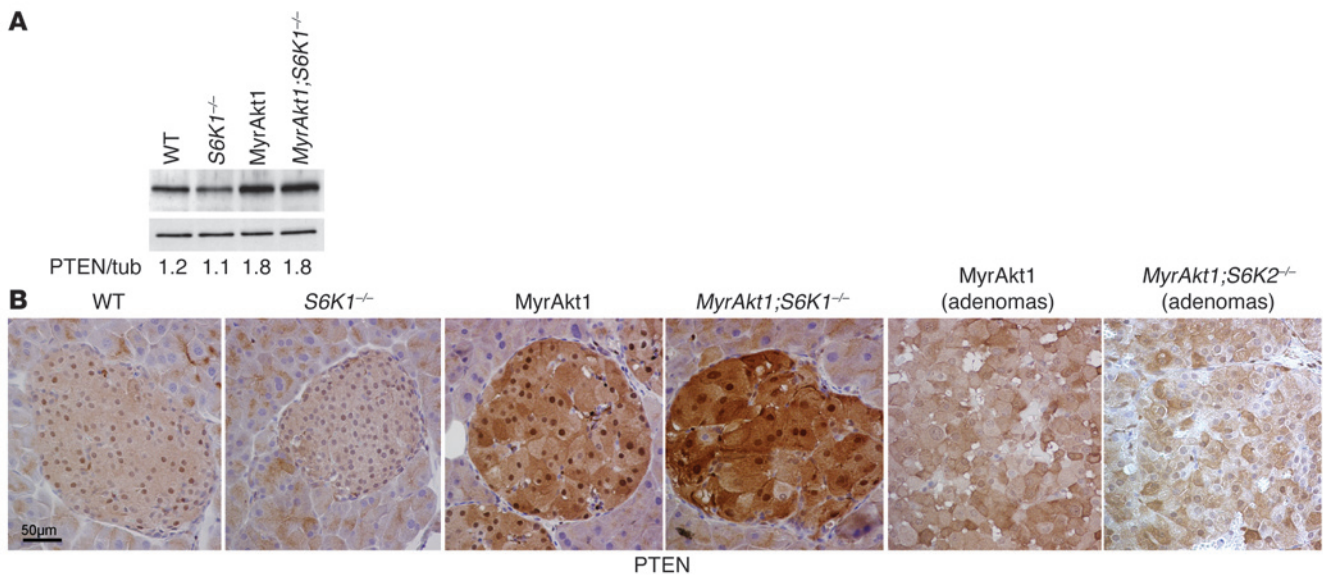
Figure 5
Increased PTEN expression in hypertrophic *RIP-MyrAkt1* islets and nuclear exclusion in tumors. (**A**) Immunoblot analysis of protein extracts from islets of the indicated genotype using anti-PTEN antibody and tubulin (tub) as a loading control. The ratio of the densitometric assay is shown. (**B**) Representative sections of pancreata immunostained with antibody against PTEN. Mice of the indicated genotype were 1 year old. Scale bar: 50 μm.

To establish whether S6K1 is required for MyrAkt1-induced tumorigenesis, we evaluated the presence of insulinomas in the 4 *MyrAkt1/S6K1* genotypes. Mice from 7 to 22 months of age were scored positive or negative based on the macroscopic presence of insulinomas measuring at least 2 mm. As expected, all wild-type and *S6K1*$^{-/-}$ mice were negative (Figure 4B and data not shown). *RIP-MyrAkt1* mice developed insulinomas with a 30% penetrance after 10 months of age (Figure 4B). Strikingly, the MyrAkt1 oncogene failed to trigger insulinoma formation in β cells lacking S6K1 activity (Figure 4B).

Mammals ubiquitously express S6K2 that also displays rpS6 kinase activity and is upregulated in S6K1-deficient mice (31). Therefore we asked whether S6K2 also participated to MyrAkt1-mediated tumorigenesis. S6K2 deletion did not alter MyrAkt1 expression (Supplemental Figure 6), though it sharply decreased rpS6 phosphorylation in islets (Figure 4C). The effect on rpS6 phosphorylation was more pronounced in *S6K2*$^{-/-}$ β cells as compared with *S6K1*$^{-/-}$ β cells, consistent with previous data in other cell types indicating S6K2 as the main rpS6 kinase in mice (24, 31, 32). Despite the inhibition of rpS6 phosphorylation, S6K2 inactivation did not impair tumor formation, which was observed in 26% of the pancreata from *MyrAkt1;S6K2*$^{-/-}$ mice between 10 and 20 months of age (Figure 4B). Thus MyrAkt1-induced tumor formation is specifically dependent on S6K1 activity in pancreatic β cells and does not correlate with rpS6 phosphorylation status.

Since the antitumoral activity of rapamycin in a number of animal models has been explained by the inhibition of HIF1α-driven angiogenesis (33, 34), we evaluated the expression of the proangiogenic HIF1α target VEGF by immunostaining analysis. Although immunostaining is not an accurate measurement of protein levels, no major differences in VEGF expression were observed among the distinct genotypes (Supplemental Figure 7A). To further address angiogenesis, capillary density was analyzed with the endothelial cell marker MECA-32. Pancreata from *RIP-MyrAkt1;S6K1*$^{-/-}$ and

RIP-MyrAkt1 mice displayed similar vascularization (Supplemental Figure 7B), indicating that angiogenesis is not the primary target of S6K1-dependent tumorigenesis.

To further dissect what growth responses were affected by S6K1 activity, we performed histochemical and morphometric analysis of pancreata between 10 and 18 months of age. The number of dysplastic lesions was similar in *RIP-MyrAkt1;S6K1*$^{-/-}$ and *RIP-MyrAkt1* mice (Supplemental Figure 8). Conversely, hyperplastic islets with a high rate of BrdU incorporation and/or malignant transformation were never observed in *RIP-MyrAkt1;S6K1*$^{-/-}$ pancreata (Figure 4A). In conclusion, S6K1 activity is not required for the MyrAkt1-induced increase in β cell size, angiogenesis, and dysplastic lesions in the pancreatic islets. However, S6K1 deletion specifically impairs tumor hyperplasia and malignancy.

Monoallelic mutations in the tumor suppressor *PTEN* gene are found in the majority of endocrine pancreatic tumors (35). We therefore evaluated PTEN expression in *RIP-MyrAkt1* islets and insulinomas. Strikingly, PTEN protein levels were increased by 50% in MyrAkt1-expressing islets independently of S6K1 activity (Figure 5A). Next, cellular distribution of PTEN was analyzed by immunohistochemistry in hypertrophic and hyperplastic islets. PTEN was localized in nucleus and cytosol of wild-type islets (Figure 5B). We revealed a sharp upregulation of PTEN expression in both compartments of hypertrophic *RIP-MyrAkt1* pancreatic β cells. Interestingly, PTEN expression in the nucleus was selectively lost in all proliferating adenomas. Tumors lacking S6K2 activity also displayed nuclear exclusion of PTEN. Of note, this cellular distribution closely resembles the one observed in the large majority of PTEN-positive human endocrine pancreatic tumors (35), adding new evidence that the *RIP-MyrAkt1* mice may represent an appropriate animal model of insulinomas. In conclusion, our data demonstrate that MyrAkt1-triggered insulinoma formation requires S6K1 activity and correlates with nuclear exclusion of the tumor suppressor PTEN.

Discussion

Expression of active Akt in pancreatic β cells of young transgenic mice increases cell size, cell survival, and insulin secretion; these 3 outcomes may be beneficial in sustaining β cell function during diabetes (this study and refs. 5, 6). However, here we show that this growth advantage is accompanied by dysplasia and uncontrolled proliferation, leading to insulinoma formation in older mice. Importantly, the mTORC1/S6K1 branch of Akt signaling is specifically required for the hyperplastic expansion of transformed β cells without affecting hypertrophy and proliferation of nontransformed β cells.

The fundamental role of the mTOR pathway in tumorigenesis is further supported by the efficacy of rapamycin in animal models of cancer with deregulated Akt activity. Treatment with rapamycin analogs decreases proliferation of PTEN mutant cancers in a variety of mouse tissues, including uterus, adrenal medulla, and smooth muscle cells (16, 17, 36, 37). In addition to this cytostatic effect, rapamycin analogs have been reported to cause regression of Akt-driven prostatic intraepithelial neoplasia due to a specific antiangiogenic and proapoptotic effect of the drug on cancer tissues (33). Although the inhibition of G1 cyclins and HIF1α expression may respectively explain the effect of rapamycin on tumor cell proliferation and survival, these are endpoints of mTOR-dependent regulation while the direct mTOR substrates that favor tumorigenesis remain to be established. Rapamycin mainly acts on mTORC1 activity, thus causing the dephosphorylation of the mTORC1 substrates S6K1/S6K2 and 4EBP1, 4EBP2, and 4EBP3. However, prolonged rapamycin treatment can also interfere with mTORC2 formation and affect Akt activity (18). Moreover, it is possible that the majority of mTOR substrates have yet to be identified. Among this broad list of putative targets, our data indicate that S6K1, but not the highly similar S6K2 protein, participates in tumor progression. Since the combined deletion of 4EBP1 and 4EBP2 does not affect tumorigenesis (38), S6K1 is the first protumoral mTORC1 substrate, to our knowledge, that has been identified. Interestingly, the *S6K1* gene is amplified in breast cancer and mutated in colorectal cancer (39, 40). Although functional studies are needed to demonstrate a growth advantage in cancer cells carrying these mutations, these data in human patients are consistent with a permissive role of S6K1 in tumorigenesis.

How S6K1 favors cancer progression is not yet known. Our data do not support a role for rpS6 phosphorylation in this process, as S6K2 deletion does not block insulinoma onset but does blunt rpS6 phosphorylation to an extent greater than that of S6K1 deletion (Figure 4C). The different phenotypes of S6K1- and S6K2-deficient mice in terms of body size, muscle and adipose tissue growth, insulin levels and sensitivity, and tumorigenesis point to isoform-specific molecular mechanisms. The existence of specific substrates has been demonstrated, as the exon-junction complex component SKAR is selectively phosphorylated by S6K1, but not S6K2 (41). Recently, the tumor suppressor PDCD4 has been shown to be ubiquitinated and degraded after phosphorylation by S6K1 (42), suggesting a mechanism for S6K1-dependent tumor formation that needs to be addressed in the future. Our findings rule out an effect of S6K1 on islet angiogenesis and dysplasia (Supplemental Figures 7 and 8) but point toward a mechanism that sustains the proliferative potential of transformed cells. We consider unlikely a direct effect of S6K1 deletion on the cell-cycle machinery, as the proliferation rate does not differ as a function of the S6K1 genotype in untransformed cells (Figure 4A) (24,

32). The incomplete penetrance and late onset of the MyrAkt1 oncogenic effect in islets suggests that additional mutations are required for transformation. One possibility is that S6K1 deletion delays the onset of these secondary mutations. Interestingly, S6K1 deletion stimulates mitochondrial biogenesis (12, 43), which might interfere with the formation of reactive oxygen species and with mutational rates. An alternative possibility is that the metabolic reprogramming in S6K1-deficient mice sharply decreases the risk of tumor formation. In skeletal muscles, we have shown that S6K1-null cells preferentially use lipids rather than glucose as energy sources and present increased respiration/glycolysis ratios (43). In humans, obese conditions and the upregulation of glycolytic pathway provide advantages for tumor growth (44). Finally, we cannot exclude the possibility that humoral effects in S6K1-deficient mice create an extracellular environment that does not favor pancreatic β cell transformation. Clearly the identification of the specific S6K1 substrate involved in tumor formation will help in addressing the contribution of these different possibilities.

Among the possible molecular mechanisms for Akt- and S6K-dependent tumorigenesis, our data suggest that nuclear exclusion of the tumor suppressor PTEN may be involved in oncogenic transformation of MyrAkt1-expressing islets. During the hypertrophic stage preceding the onset of insulinomas, PTEN expression is sharply upregulated in both nucleus and cytosol of *RIP-MyrAkt1* pancreatic β cells, indicating that PTEN may be required to keep under control cell-cycle progression and chromosomal integrity in cells expressing the MyrAkt1 oncogene. The hyperplastic transformation of MyrAkt1-expressing adenomas tightly correlates with a selective loss of nuclear PTEN, as observed for other tumors (45). Presently, we cannot determine whether PTEN nuclear exclusion in pancreatic β cells is a cause or a consequence of cell transformation. Previous studies have demonstrated that the function of nuclear PTEN is essential for tumor suppression (45). Despite this functional relevance, the regulation of nucleocytoplasmic shuttling remains to be elucidated. PTEN lacks classical nuclear localization sequences (NLSs) or nuclear export sequences, though NLS-like and nuclear exclusion sequences have been reported. In addition, mono- and polyubiquitination also participate in nuclear transport. Of note, the Akt/mTOR/S6K pathway has been proposed to directly regulate cellular distribution of PTEN (46). Rapamycin and S6K1/S6K2 knockdown suppress nuclear export of PTEN in cultured cells. S6K1 can interact with and phosphorylate in vitro PTEN, though in vivo evidence is still lacking. These findings suggest a potential mechanism to explain the dependency on S6K for oncogenesis in our system. Since we were unable to reveal differential localization of PTEN in *RIP-MyrAkt1;S6K1^{-/-}* and *RIP-MyrAkt1* islets during the hypertrophic stage, it is possible that additional factors cooperate with S6K in the regulation of PTEN during transformation. The relevance of these observations for human tumors is outlined by the findings that monoallelic mutations and nuclear exclusion of PTEN are commonly observed in human samples of pancreatic endocrine neoplasia (35).

Insulinomas in humans are rare tumors that represent around 1% of all pancreatic neoplasms. The somatic mutations leading to insulinoma formation are not firmly established, though PTEN loss of function may represent a likely candidate, as previously described (35). Of note, inherited mutations in the multiple endocrine neoplasia type 1 (*MEN1*), von Hippel–Lindau (*VHL*), neurofibromatosis type 1 (*NF1*), and *TSC1/2* genes

predispose to the development of endocrine pancreatic cancers (47). Interestingly, rapamycin derivatives are extremely effective as therapeutic agents to treat VHL, NF1, and TSC syndromes in human patients or animal models of the disease (34, 48, 49). These findings in combination with our data point to the activation of the mTOR pathway as a frequent event required for endocrine pancreatic cancer development.

Based on their clinical manifestations, endocrine pancreatic cancers are subdivided into functioning and nonfunctioning tumors. Functioning tumors are more common and usually benign, as clinical manifestations allow a rapid diagnosis. In the case of insulinomas, they are life threatening due to hyperinsulinemia and the resulting hypoglycemic disturbances. In the large majority of *RIP-MyrAkt1* mice, insulinoma cells are functional, as they maintain insulin expression and secretion (Figure 3). We have observed several times that, in contrast with other animal models of insulinomas (50, 51), *RIP-MyrAkt1* mice with relatively small tumors may die of hypoglycemia, indicating that most MyrAkt1-expressing β cells remain well differentiated. However, we also have found a small percentage of insulin-negative malignant carcinomas among the tumor specimens, demonstrating that MyrAkt1 can also accelerate the course of nonfunctioning tumors. Thus, the *RIP-MyrAkt1* mice recapitulate relevant features of insulinoma formation in humans and represent an attractive model to address etiology and therapeutic intervention.

The Akt/mTOR-signaling pathway is emerging as a master regulator of multiple pancreatic β cell functions, from insulin synthesis to insulin secretion, β cell survival, neogenesis, proliferation, size, and transformation. The dissection of the specific Akt/mTOR branches affecting one function but not others is clearly relevant for therapy. By showing that S6K1 gene deletion selectively impairs β cell transformation, our results suggest strategies to maintain cell physiology while minimizing cancer risks.

Methods

Animals. Generation of RIP-MyrAkt1–expressing mice as well as *S6K1-* and *S6K2*-deficient mice has been previously described (5, 31, 32). *RIP-MyrAkt1* transgenic and *S6K*-deficient mouse lines were backcrossed to a C57BL/6 genetic background for 6 or 8 generations, respectively. Since the combined mutation of S6K1 and S6K2 was lethal in the C57BL/6 genetic background, *RIP-MyrAkt1;S6K1$^{-/-}$;S6K2$^{-/-}$* mice had a mixed background and were compared with littermates not carrying the *RIP-MyrAkt1* transgene. Mice were maintained at 22°C with a 12-hour dark/12-hour light cycle and had free access to food. All animal studies were approved by the Direction Départementale des Services Vétérinaires, Prefecture de Police, Paris, France (authorization number 75-1313).

Metabolic studies. At 2 months, a glucose tolerance test was performed after an overnight fast (14 hours). Mice were i.p. injected with 2 g/kg glucose, and blood was collected from the tail veins for determination of glucose levels at 0, 15, 30, 45, and 100 minutes by Glucotrend glucometer (Roche). To test for insulin resistance, at 3 months, an insulin tolerance test was performed. Overnight-fasted mice were i.p. injected with 1 U/kg insulin (Actrapid; Novo Nordisk), and the glucose concentration in whole blood from the tail veins was measured at 0, 15, 30, and 60 minutes. Fasting insulin levels were measured by ELISA (Crystal Chem Inc.).

Immunohistochemistry. Pancreatic tissue was fixed overnight in 4% paraformaldehyde solution and embedded in paraffin, sectioned in 5 μm slices, and stained either with H&E or, for trichrome staining, with fuchsin acid and anilin blue. Immunohistochemistry was performed with the following antibodies: anti–phospho-Ser235/236 S6 antibody

(Cell Signaling Technology); anti-Glut2 antibody (Alpha Diagnostic International); anti-HA antibody (Roche); anti-BrdU antibody (Roche); anti-insulin antibody (Linco); anti-VEGF antibody (R&D Systems); anti-PTEN antibody (Cell Signaling Technology);, anti-β catenin antibody (BD Biosciences); and anti-PDX1 antibody (generous gift of Raphael Scharfmann). For immunostaining with anti–MECA-32 antibody (BD Biosciences), frozen sections were used.

Western blot. Tissue was lysed in 20 mM Tris-HCl (pH 8.0), 5% glycerol, 138 mM NaCl, 2.7 mM KCl, 1% NP-40, 20 mM NaF, 5 mM EDTA, 1 mM sodium orthovanadate, 5 μg/ml leupeptin, 1 μg/ml pepstatin, and 1 mM DTT. To remove cell debris, homogenates were spun at 8000 g for 10 minutes at 4°C. Protein extract from pancreas was resolved by SDS-PAGE before transfer onto nitrocellulose membrane and incubation with the anti–phospho-Ser473 Akt primary antibody, anti-PTEN antibody, anti–4EBP1 antibody, anti–phospho-Ser9 GSK3 antibody (Cell Signaling Technology Inc.), and anti-tubulin antibody (Sigma-Aldrich). To estimate the levels of phosphorylation of GSK3, 4EBP1, and PTEN expression reported to tubulin, densitometry was performed using ImageJ software (http://rsbweb.nih.gov/ij/).

Islet isolation. Islet isolation was accomplished by collagenase P (4.3 U/mg; Roche) digestion for 8 minutes at 37°C. After 3 sequential washes, digested tissue was layered over 10 ml of histopaque (Sigma-Aldrich) and spun for 15 minutes at increasing speeds (from 50 to 900 g). Islets were hand picked and incubated overnight in RPMI medium with 20 mM glucose. Then islets were lysed in Tris/HCl, pH 6.8, 1 M, 1% SDS and boiled for 5 minutes at 100°C.

Morphometric analysis. β cell size measurement was performed with LUCIA software on Glut2 and HA coimmunostaining of sections from 4-month-old mice. Only the HA-positive β cell size was measured in the MyrAkt1 genotype. At least 200 β cells from 10 distinct islets were analyzed per mouse. β cell proliferation was determined by BrdU incorporation. Mice were injected i.p. with 50 mg/kg of BrdU and sacrificed after 8 hours. The results were expressed as the ratio between islet BrdU-positive cells and the islet area from 1-year-old mouse pancreatic sections. At least 20 islets were analyzed. Endocrine surface was assessed by insulin immunostaining using ImageJ software and expressed over the total pancreas surface. The number of dysplastic islets in 1-year-old mice was expressed as a percentage over the total number of islets in the pancreas area of at least 40 mm².

Statistics. Analysis was performed by 2-tailed, unpaired Student's *t* test. *P* values of less than 0.05 were considered significant.

Address correspondence to: Mario Pende, INSERM U845, 156 rue de Vaugirard, Paris F-75015, France. Phone: 33-1-40-61-53-15, Fax: 33-1-43-06-04-43; E-mail: mario.pende@inserm.fr.

1. Kulkarni, R.N. 2005. New insights into the roles of insulin/IGF-I in the development and maintenance of beta-cell mass. *Rev. Endocr. Metab. Disord.* **6**:199–210.

2. Ueki, K., et al. 2006. Total insulin and IGF-I resistance in pancreatic beta cells causes overt diabetes. *Nat. Genet.* **38**:583–588.

3. Withers, D.J., et al. 1999. Irs-2 coordinates Igf-1 receptor-mediated beta-cell development and peripheral insulin signalling. *Nat. Genet.* **23**:32–40.

4. Pende, M., et al. 2000. Hypoinsulinaemia, glucose intolerance and diminished beta-cell size in S6K1-deficient mice. *Nature.* **408**:994–997.

5. Tuttle, R.L., et al. 2001. Regulation of pancreatic beta-cell growth and survival by the serine/threonine protein kinase Akt1/PKBalpha. *Nat. Med.* **7**:1133–1137.

6. Bernal-Mizrachi, E., Wen, W., Stahlhut, S., Welling, C.M., and Permutt, M.A. 2001. Islet beta cell expression of constitutively active Akt1/PKB alpha induces striking hypertrophy, hyperplasia, and hyperinsulinemia. *J. Clin. Invest.* **108**:1631–1638.

7. Bhaskar, P.T., and Hay, N. 2007. The two TORCs and Akt. *Dev. Cell.* **12**:487–502.

8. Harada, H., Andersen, J.S., Mann, M., Terada, N., and Korsmeyer, S.J. 2001. p70S6 kinase signals cell survival as well as growth, inactivating the pro-apoptotic molecule BAD. *Proc. Natl. Acad. Sci. U. S. A.* **98**:9666–9670.

9. Zhang, H.H., Lipovsky, A.I., Dibble, C.C., Sahin, M., and Manning, B.D. 2006. S6K1 regulates GSK3 under conditions of mTOR-dependent feedback inhibition of Akt. *Mol. Cell.* **24**:185–197.

10. Kim, D.H., et al. 2002. mTOR interacts with raptor to form a nutrient-sensitive complex that signals to the cell growth machinery. *Cell.* **110**:163–175.

11. Sarbassov, D.D., Guertin, D.A., Ali, S.M., and Sabatini, D.M. 2005. Phosphorylation and regulation of Akt/PKB by the rictor-mTOR complex. *Science.* **307**:1098–1101.

12. Um, S.H., et al. 2004. Absence of S6K1 protects against age- and diet-induced obesity while enhancing insulin sensitivity. *Nature.* **431**:200–205.

13. Manning, B.D., and Cantley, L.C. 2003. Rheb fills a GAP between TSC and TOR. *Trends Biochem. Sci.* **28**:573–576.

14. Ma, L., et al. 2005. Genetic analysis of Pten and Tsc2 functional interactions in the mouse reveals asymmetrical haploinsufficiency in tumor suppression. *Genes Dev.* **19**:1779–1786.

15. Manning, B.D., et al. 2005. Feedback inhibition of Akt signaling limits the growth of tumors lacking Tsc2. *Genes Dev.* **19**:1773–1778.

16. Neshat, M.S., et al. 2001. Enhanced sensitivity of PTEN-deficient tumors to inhibition of FRAP/mTOR. *Proc. Natl. Acad. Sci. U. S. A.* **98**:10314–10319.

17. Podsypanina, K., et al. 2001. An inhibitor of mTOR reduces neoplasia and normalizes p70/S6 kinase activity in Pten⁺/⁻ mice. *Proc. Natl. Acad. Sci. U. S. A.* **98**:10320–10325.

18. Sarbassov, D.D., et al. 2006. Prolonged rapamycin treatment inhibits mTORC2 assembly and Akt/PKB. *Mol. Cell.* **22**:159–168.

19. Whiteman, E.L., Cho, H., and Birnbaum, M.J. 2002. Role of Akt/protein kinase B in metabolism. *Trends Endocrinol. Metab.* **13**:444–451.

20. Vivanco, I., and Sawyers, C.L. 2002. The phosphatidylinositol 3-Kinase AKT pathway in human cancer. *Nat. Rev. Cancer.* **2**:489–501.

21. Luo, J., Manning, B.D., and Cantley, L.C. 2003. Targeting the PI3K-Akt pathway in human cancer: rationale and promise. *Cancer Cell.* **4**:257–262.

22. Manning, B.D., and Cantley, L.C. 2007. AKT/PKB signaling: navigating downstream. *Cell.* **129**:1261–1274.

23. Giordano, E., et al. 1993. B-cell size influences glucose-stimulated insulin secretion. *Am. J. Physiol.* **265**:C358–C364.

24. Ohanna, M., et al. 2005. Atrophy of S6K1(–/–) skeletal muscle cells reveals distinct mTOR effectors for cell cycle and size control. *Nat. Cell Biol.* **7**:286–294.

25. Rommel, C., et al. 2001. Mediation of IGF-1-induced skeletal myotube hypertrophy by PI(3)K/Akt/mTOR and PI(3)K/Akt/GSK3 pathways. *Nat. Cell Biol.* **3**:1009–1013.

26. Sandri, M., et al. 2004. Foxo transcription factors induce the atrophy-related ubiquitin ligase atrogin-1 and cause skeletal muscle atrophy. *Cell.* **117**:399–412.

27. Fingar, D.C., Salama, S., Tsou, C., Harlow, E., and Blenis, J. 2002. Mammalian cell size is controlled by mTOR and its downstream targets S6K1 and 4EBP1/eIF4E. *Genes Dev.* **16**:1472–1487.

28. Manning, B.D., and Cantley, L.C. 2003. United at last: the tuberous sclerosis complex gene products connect the phosphoinositide 3-kinase/Akt pathway to mammalian target of rapamycin (mTOR) signalling. *Biochem. Soc. Trans.* **31**:573–578.

29. Marr, M.T., D'Alessio, J.A., Puig, O., and Tjian, R. 2007. IRES-mediated functional coupling of transcription and translation amplifies insulin receptor feedback. *Genes Dev.* **21**:175–183.

30. Leibiger, I.B., Leibiger, B., Moede, T., and Berggren, P.O. 1998. Exocytosis of insulin promotes insulin gene transcription via the insulin receptor/PI-3 kinase/p70 s6 kinase and CaM kinase pathways. *Mol. Cell.* **1**:933–938.

31. Shima, H., et al. 1998. Disruption of the p70(s6k)/p85(s6k) gene reveals a small mouse phenotype and a new functional S6 kinase. *EMBO J.* **17**:6649–6659.

32. Pende, M., et al. 2004. S6K1(–/–)/S6K2(–/–) mice exhibit perinatal lethality and rapamycin-sensitive 5′-terminal oligopyrimidine mRNA translation and reveal a mitogen-activated protein kinase-dependent S6 kinase pathway. *Mol. Cell. Biol.* **24**:3112–3124.

33. Majumder, P.K., et al. 2004. mTOR inhibition reverses Akt-dependent prostate intraepithelial neoplasia through regulation of apoptotic and HIF-1–dependent pathways. *Nat. Med.* **10**:594–601.

34. Thomas, G.V., et al. 2006. Hypoxia-inducible factor determines sensitivity to inhibitors of mTOR in kidney cancer. *Nat. Med.* **12**:122–127.

35. Perren, A., et al. 2000. Mutation and expression analyses reveal differential subcellular compartmentalization of PTEN in endocrine pancreatic tumors compared to normal islet cells. *Am. J. Pathol.* **157**:1097–1103.

36. Wendel, H.G., et al. 2004. Survival signalling by Akt and eIF4E in oncogenesis and cancer therapy. *Nature.* **428**:332–337.

37. Hernando, E., et al. 2007. The AKT-mTOR pathway plays a critical role in the development of leiomyosarcomas. *Nat. Med.* **13**:748–753.

38. Le Bacquer, O., et al. 2007. Elevated sensitivity to diet-induced obesity and insulin resistance in mice lacking 4E-BP1 and 4E-BP2. *J. Clin. Invest.* **117**:387–396.

39. Barlund, M., et al. 2000. Multiple genes at 17q23 undergo amplification and overexpression in breast cancer. *Cancer Res.* **60**:5340–5344.

40. Wood, L.D., et al. 2007. The genomic landscapes of human breast and colorectal cancers. *Science.* **318**:1108–1113.

41. Ma, X.M., Yoon, S.O., Richardson, C.J., Julich, K., and Blenis, J. 2008. SKAR links pre-mRNA splicing to mTOR/S6K1-mediated enhanced translation efficiency of spliced mRNAs. *Cell.* **133**:303–313 .

42. Dorrello, N.V., et al. 2006. S6K1- and bTRCP-mediated degradation of PDCD4 promotes protein translation and cell growth. *Science.* **314**:467–471.

43. Aguilar, V., et al. 2007. S6 kinase deletion suppresses muscle growth adaptations to nutrient availability by activating AMP kinase. *Cell Metab.* **5**:476–487.

44. Thompson, C.B., et al. 2005. How do cancer cells acquire the fuel needed to support cell growth? *Cold Spring Harb. Symp. Quant. Biol.* **70**:357–362.

45. Salmena, L., Carracedo, A., and Pandolfi, P.P. 2008. Tenets of PTEN tumor suppression. *Cell.* **133**:403–414.

46. Liu, J.L., et al. 2007. Cell cycle-dependent nuclear export of phosphatase and tensin homologue tumor suppressor is regulated by the phosphoinositide-3-kinase signaling cascade. *Cancer Res.* **67**:11054–11063.

47. Jonkers, Y.M., Ramaekers, F.C., and Speel, E.J. 2007. Molecular alterations during insulinoma tumorigenesis. *Biochim. Biophys. Acta.* **1775**:313–332.

48. Johannessen, C.M., et al. 2008. TORC1 is essential for NF1-associated malignancies. *Curr. Biol.* **18**:56–62.

49. Paul, E., and Thiele, E. 2008. Efficacy of sirolimus in treating tuberous sclerosis and lymphangioleiomyomatosis. *N. Engl. J. Med.* **358**:190–192.

50. Lopez, T., and Hanahan, D. 2002. Elevated levels of IGF-1 receptor convey invasive and metastatic capability in a mouse model of pancreatic islet tumorigenesis. *Cancer Cell.* **1**:339–353.

51. Pelengaris, S., Khan, M., and Evan, G.I. 2002. Suppression of Myc-induced apoptosis in beta cells exposes multiple oncogenic properties of Myc and triggers carcinogenic progression. *Cell.* **109**:321–334.